

Modelling of beam-driven high frequency Alfvén eigenmodes in MAST

M K Lilley¹, S E Sharapov², H M Smith³, R J Akers², D McCune⁴ and The MAST team²

¹*Physics Department, Imperial College, London, SW7 2AZ, UK*

²*EURATOM/UKAEA Fusion Association, Culham Science Centre, Abingdon, OX14 3DB, UK*

³*Physics Department, University of Warwick, Coventry, CV4 7AL, UK*

⁴*PPPL, Princeton University, Princeton, New Jersey 08543, USA*

Introduction: Alfvén eigenmodes (AEs) are studied due to the potential redistribution of fast ions that they can cause and also for the purpose of diagnosing plasma parameters [1]. Modes driven by both the radial gradient of the fast ion pressure, e.g. Toroidal Alfvén Eigenmodes (TAEs) [2], and by energy space gradients, e.g. Compressional Alfvén Eigenmodes (CAEs) [3], have been previously studied on NSTX [4] and observed on MAST [5], driven by super Alfvénic ions produced by neutral beam injection (NBI) [6, 7]. For instabilities with frequency ω comparable to the ion cyclotron frequency Ω_i , the relevant fast particle resonance responsible for the mode excitation is the Doppler shifted cyclotron resonance [8],

$$\omega - k_{\parallel} v_{\parallel \text{res}} - l \Omega_b = 0 \quad (1)$$

where $k_{\parallel} = \mathbf{k} \cdot \mathbf{B}_0 / |\mathbf{B}_0|$, l is an integer, $l = +1$ corresponds to the Doppler resonance, $l = -1$ corresponds to the anomalous Doppler resonance and $v_{\parallel \text{res}}$ is the parallel velocity of the resonant beam particles. Note on MAST the NBI and thermal plasma ions are both deuterium so that $\Omega_b = \Omega_D$. New MAST data [9], obtained using high power super Alfvénic NBI, shows significant AE activity in the ion cyclotron frequency range with the intermediate frequency modes having a large compressional component [10]. The aim of the present paper is to perform kinetic modelling of the linear drive and damping for global AEs. A 1-D model [11, 12] for computing AEs is used with the NBI distribution function computed using the TRANSP code [13]. The 1-D eigenmode model is simpler than the models from Refs. [14, 4], but allows extensive parameter space scans of toroidal mode number and k_{\parallel} .

Experimental data: MAST is a small aspect ratio spherical tokamak (ST) with major and minor radii of $R_0 = 0.86\text{m}$ and $a = 0.6\text{m}$ respectively. In a recent series of MAST discharges, with co- I_p NBI with $E_{\text{NBI}}^{\text{max}} \approx 65\text{keV}$ and $v_{\parallel b}^{\text{max}}/v_A \approx 2.5$, we observed persistent AEs which span a frequency range between $\Omega_D(R_0)/4$ and just above $\Omega_D(R_0) \approx 2.3 \times 10^7 \text{rads}^{-1}$ ($f_{cD} \approx 3.6\text{MHz}$) (where $\Omega_D(R_0)$ is the cyclotron frequency at the geometric axis). Figures 1 - 3 show a typical example of such data.

Figure 2 shows toroidal mode numbers (n) of the AEs, which are only negative and decrease in frequency as $|n|$ increases ($n < 0$ implies counter I_p). The fine frequency splitting between successive mode numbers can be explained by toroidal plasma rotation $f_{\text{rot}}^{\text{max}} \approx 19\text{kHz}$, driven by NBI. However, this rotation cannot explain large frequency separations e.g. $\Delta f_{n=-5 \rightarrow -6} \approx 150\text{kHz}$. It is important to note that AEs with a maximum frequency of 3.8MHz , exceeding the cyclotron frequency $f_{cD}(R_0) = 3.77\text{MHz}$, were observed in pulse #18886 (not shown).

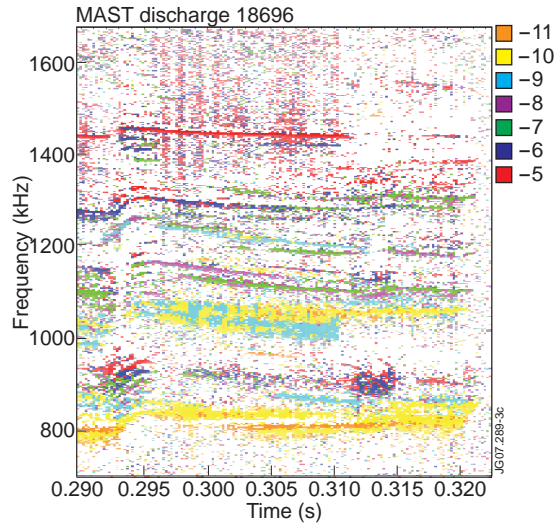


Figure 2: Toroidal mode number (n) analysis. Here we see high negative mode numbers.

Modelling the NBI distribution function: Using TRANSP [13] with 10^5 macro particles the deuterium NBI distribution function at $t = 0.32\text{s}$ has been calculated, which shows that most of the NBI produced ions are deposited in the core. Figure 4 shows that a high density bump on tail in NBI energy exists, due to the balance of charge exchange losses at lower energy and beam sources at high energy, out to a normalised radius of $r/a = 0.425$, where $n_0 = 4 \times 10^{19}\text{m}^{-3}$, $T = 950\text{eV}$, $n_b = 5 \times 10^{17}\text{m}^{-3}$.

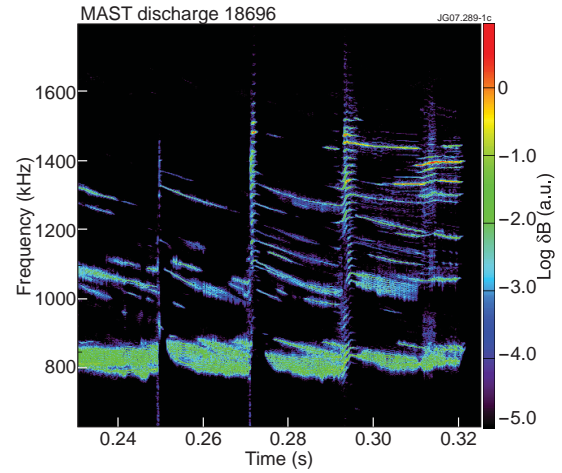


Figure 1: Spectrogram of AEs from Mirnov coils on MAST pulse 18696

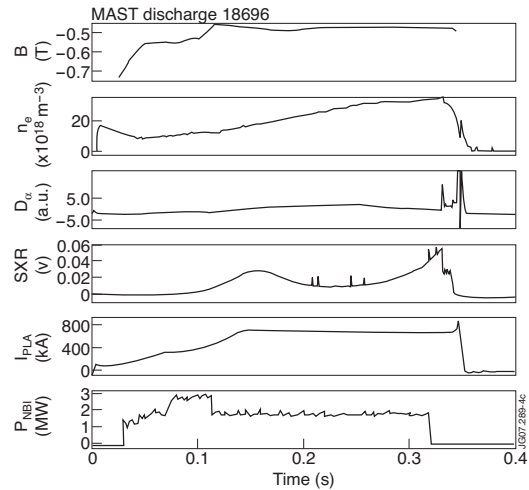
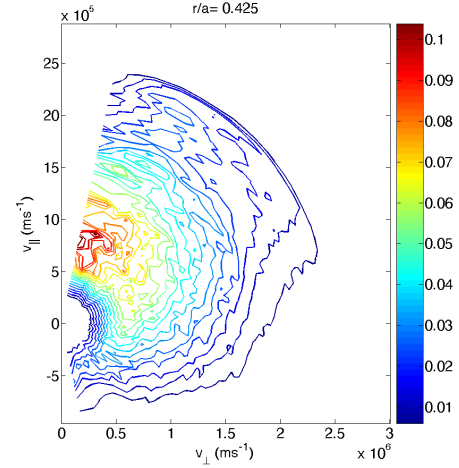


Figure 3: Evolution of vacuum field, electron density, D_α signal, soft X-ray, plasma current and NBI power.

A shifted Gaussian distribution in velocity space can represent the NBI distribution function in the relevant phase space region,

$$f_b = \frac{n_b e^{-(v_{\parallel} - v_{\parallel b})^2 / \Delta v_{\parallel}^2} e^{-(v_{\perp} - v_{\perp b})^2 / \Delta v_{\perp}^2}}{2\pi^2 v_{\perp b} \Delta v_{\perp} \Delta v_{\parallel}} \quad (2)$$

with following NBI parameters (which are fitted to the TRANSP result) $v_{\perp b} = 6 \times 10^6 \text{ms}^{-1}$, $v_{\parallel b} = -1.47 \times 10^6 \text{ms}^{-1}$, $\Delta v_{\perp} = 1 \times 10^5 \text{ms}^{-1}$ and $\Delta v_{\parallel} = 1.03 \times 10^5 \text{ms}^{-1}$. We will assume $v_{\perp b}^2 \gg \Delta v_{\perp}^2$ in all calculations that follow.



Global kinetic analysis: In order to calculate the global linear kinetic drive, γ^{gl} , associated with the NBI distribution function in Eq. (2) and Maxwellian thermal plasma species, we perform the following weighted integral of the local kinetic drive and damping, γ^{loc} , with the wave electric field ($E(r)$) over the region of the eigenmode localisation [3]

$$\gamma^{\text{gl}} = \frac{\int_0^a r dr \gamma^{\text{loc}}(r) |E(r)|^2}{\int_0^a |E(r)|^2}. \quad (3)$$

where, for small k_{\perp} , the NBI contribution to γ^{loc} takes the following form

$$\frac{\gamma^{\text{loc}}}{\omega} = \frac{-\sqrt{\pi} e^{-x_{\mp}^2} \frac{\omega_{pb}^2}{\omega} \left[\frac{1}{k_{\parallel} \Delta v_{\parallel}} - \frac{v_{\parallel b}}{\Delta v_{\parallel} \omega} + x_{\mp} \left(-\frac{1}{\omega} + \frac{3}{2} \frac{\Delta v_{\perp}^2}{\Delta v_{\parallel}^2} + \frac{v_{\perp b}^2}{\Delta v_{\parallel}^2} \right) \right] \text{sgn}(k_{\parallel})}{2 + \frac{\omega_{pD}^2}{(\omega \mp \Omega_D)^2}}, \quad x_{\mp} = \frac{\omega - k_{\parallel} v_{\parallel b} \mp \Omega_D}{k_{\parallel} \Delta v_{\parallel}} \quad (4)$$

We use a 1-D ‘hollow cylinder’ model [12] for calculating a discrete spectrum of AEs in the frequency range compatible with the experimental observations and use the Doppler resonance condition from Eq. 1 to identify the resonant particle velocity for a given eigenmode. As a result of the eigenmode analysis, we obtain $E(r)$ and the global drive given by Eq 3. For the NBI distribution function given by Eq. 2 the value of the drive is sensitive with respect to $v_{\parallel b}$ and $v_{\perp b}$. In order to assess this sensitivity we vary $v_{\parallel b}$ and $v_{\perp b}$ within the TRANSP error bars (of about 10%) for a mode with $n = -9$, $k_{\parallel} = 6.8 \text{m}^{-1}$ and $f \approx 1 \text{MHz}$ (Fig. 5).

The maximum growth rate calculated within the TRANSP error bars is between $\gamma^{\text{gl}}/\omega \approx 0.1\%$ and 1% which is then consistent with experimentally measured linear growth rate of $\gamma^{\text{gl}}/\omega = 0.5\%$.

Absence of $n > 0$ modes: The observed $n < 0$ modes were driven via the Doppler resonance, $l = +1$ in Eq. 1, while the $n > 0$ modes can only be driven via the anomalous Doppler resonance, $l = -1$. Although the NBI on MAST was super Alfvénic, it was still below the critical beam speed required for exciting the right hand polarised compressional Alfvén eigenmodes (CAEs),

$$v_{\parallel b} > \frac{3\sqrt{3}}{2}v_A. \quad (5)$$

The validity of Eq. 5 can be tested experimentally by lowering the magnetic field.

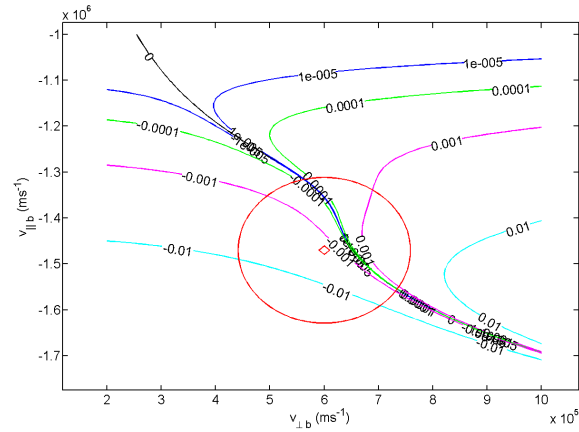


Figure 5: γ^l/ω contours as a function of $v_{\parallel b}$ and $v_{\perp b}$. The red circle shows the 10% tolerance around the TRANSP value of the modelled beam velocity.

Conclusions: It is now be understood that high frequency AEs on MAST are driven via the Doppler shifted cyclotron resonance condition by a bump on tail free energy source associated with the NBI ions. The absence of $n > 0$ AEs can now be understood to be a result of the existence of a critical beam velocity, which was not exceeded experimentally.

Acknowledgements: We would like to acknowledge to help of M. P. Gryaznevich, S. D. Pinches and L. C. Appel. This work was partly funded by the UK Engineering and Physical Sciences Research Council and the European Communities under the contract of Association between EURATOM and UKAEA.

References: [1] S. E. Sharapov, Nuclear Fusion, 45:1168-1177, 2005. [2] C. Z. Cheng and L. Chen, Annals of Physics, 161(1):21-47, 1985. [3] B. Coppi, Physics of Fluids, 12(12):4060, 1986. [4] N. N. Gorelenkov, Nuclear Fusion, 42:997-985, 2002. [5] L. C. Appel, submitted to PPCF (2008), number P-4.195, 2004. [6] B. Lloyd, Nuclear Fusion, 43:1665. [7] E. D. Fredrickson, Physics of Plasmas, 10:2852, 2003. [8] A. I. Akhiezer, Plasma Electrodynamics Volume 1: Linear Theory. Pergamon Press, 1975. [9] M. P. Gryaznevich, 10th IAEA Meeting on Energetic Particles, Kloster Seon, 2007. [10] R. Vann, 10th IAEA Meeting on Energetic Particles, Kloster Seon, 2007. [11] M. K. Lilley, Physics of Plasmas, 14:082501, 2007. [12] V. D. Yegorenkov, K. N. Stepanov, In 17th EPS, volume 3, page 1207, Venice, 1989. [13] R. Budny, Nuclear Fusion, 32:429, 1992. [14] H. Smith, Physics of Plasmas, 10(5):1427, 2003.